Electric and magnetic polarizability of Goldstone pions to subleading $\mathcal{O}(N_c^{-1})$ in the bosonized Nambu–Jona-Lasinio model

C. A. Wilmot
St. Stithians College, Private Bag 2, Randburg 2125, South Africa

R. H. Lemmer
Nuclear and Particle Theory Group, University of the Witwatersrand, Johannesburg, Private Bag 3, WITS 2050, South Africa

(Received 2 August 2001; published 4 March 2002)

We study the electric and magnetic polarizability coefficients to subleading order in the inverse number of colors N_c^{-1} by constructing Compton scattering amplitudes derived from a bosonized version of the Nambu–Jona-Lasinio (NJL) chiral Lagrangian with finite pion size effects included. We confirm the leading in N_c^{-1} mean-field results of Bajc *et al.* [Nucl. Phys. **A604**, 406 (1996)] to $\mathcal{O}(m_\pi^2)$ in the pion mass m_π. The subleading corrections arise from a gauge invariant sum of meson one-loop diagrams which is nonanalytic in m_π^2, but free of any chiral or ultraviolet divergences. These corrections lead to a $\gtrsim 30\%$ reduction in the mean-field values for the polarizability coefficients of the charged pion. Use of the sum rule estimate for the NJL quark mass renders these calculations parameter free, and dependent only on the physical observables of the pion.

DOI: 10.1103/PhysRevC.65.035206 PACS number(s): 11.30.Rd, 11.10.Lm, 11.10.St

I. INTRODUCTION

The electric and magnetic polarizability coefficients α_π and β_π of the pion characterize the long-wavelength behavior of the photon-pion Compton scattering amplitude. Near threshold this takes the form [1]

$$f_C = -\frac{e^2}{M_\pi}(\vec{\epsilon}_1\cdot\vec{\epsilon}_2)\,\delta_{T_3,\pm 1} + \alpha_\pi \omega_1 \omega_2 (\vec{\epsilon}_1\cdot\vec{\epsilon}_2) + \beta_\pi (\vec{\epsilon}_1\times\vec{q}_1)\cdot(\vec{\epsilon}_2\times\vec{q}_2) + \cdots . \quad (1)$$

Here $(\omega_i, \vec{q}_i)$ $(i=2,1)$ are the energy and momentum for incoming and outgoing photons of polarizations $\epsilon_i = (0, \vec{\epsilon}_i)$ in the transverse gauge, M_π and T_3 are the pions' mass and isospin projection, and $e^2 = \alpha \approx 1/137$. As has become customary, these coefficients will be given in (Gaussian) units of 10^{-4} fm^3.

The polarizability coefficients are fundamental parameters in pion physics. Their measurement and calculation provide important tests for pionic structure as studied in QCD, or from various effective models of the pion. These coefficients have been extracted from radiative pion photoproduction [2], radiative pion nucleus scattering [3,4], and from the crossed channel of $\gamma\gamma \to \pi\pi$ experiments [5–7]. The actual experimental values are still very uncertain, however [8,9]. On the theoretical side, their calculation has been attempted using a variety of approaches, viz., various quark models [10–18] of the pion, chiral perturbation theory (CHPT) [19–23], dispersion sum rules [24,25], and the Das-Mathur-Okubo (DMO) sum rule [26] combined with either model [1,27], empirical [28], experimental [29], QCD sum rule [30], or QCD lattice determinations of spectral densities [31]. Due to its method of derivation from current algebra the DMO sum rule option is, however, restricted to yielding charged pion polarizabilities in the chiral limit only.

According to Eq. (1), a knowledge of the Compton scattering amplitude near threshold is sufficient for computing polarizability coefficients. Classically this corresponds to examining the response of the system to electromagnetic fields that are practically constant over the dimensions of the target. The construction of Compton scattering amplitudes cannot be done exactly. Some form of perturbation approach has to be employed. In the case of CHPT a loop expansion that corresponds to a series of increasing powers of momenta is used to express the Compton scattering amplitude in terms of the empirical coupling constants of CHPT that can then be inferred from independent experimental data. Calculations up to two loops for both neutral [9] and charged pion [22,23] polarizability coefficients are available. As two-loop expansions already require an evaluation of a large number of additional diagrams ($\gtrsim 100$ diagrams for the charged channel, for example), an extension to higher-order loops is limited by the technical feasibility.

Alternatively, model Lagrangians have been constructed that attempt to mimic the breaking of the underlying chiral symmetry of QCD, with the accompanying generation of isovector pseudoscalar Goldstone bosons. These bosons are then identified with physical pions that are allowed to interact with a photon gauge field. In this regard the Nambu–Jona-Lasinio (NJL) [32,33] model has been studied in some detail in both its minimal SU(2) [16] and SU(3) [12] versions, as well as an extended SU(2) version (ENJL) that includes vector and axial vector meson modes [15]. While it was recently shown that it is possible to carry out calculations of the Compton amplitude for the minimal NJL model to all orders of external momenta [16], these calculations have been limited to a mean-field approach, characterized by keeping only leading in N_c^{-1} contributions in a series expansion in the inverse number of colors. But these calculations are already technically very complicated, requiring the use of computer-assisted validation of the Dirac traces. This in turn

suggests that the computation of terms involving single π and σ meson loops generated self-consistently by the NJL model (these give the subleading in N_c^{-1} contributions) to all orders in momenta will become prohibitive, and one has to resort to some approximate way for including such additional terms. In Ref. [16], for example, the authors argued for an ad hoc incorporation of the lowest order $\mathcal{O}(p^4)$ meson loop correction taken from CHPT [11] in the neutral channel scattering amplitude, but not in the charged channel, the reason being that the leading in N_c^{-1} NJL model contribution only starts at $\mathcal{O}(p^6)$ in the former channel, but already at $\mathcal{O}(p^4)$ in the latter.

In the present study we adopt a complementary point of view by using the minimal NJL model in its bosonized version from the start to generate both leading and subleading in N_c^{-1} contributions to the Compton scattering amplitude from a common Lagrangian. A particular advantage of the bosonized, or effective, NJL model Lagrangian of Ebert and Volkov [34,35] is that it explicitly puts into evidence the role of the inverse number of colors as a coupling parameter between bosonic modes with which to classify a perturbation scheme. However, this comes at a price. The leading in N_c^{-1} piece of this Lagrangian now involves a series expansion in space-time derivatives of these boson fields. In the language of Ref. [16] this regenerates their closed-form Compton scattering amplitudes in the form of power series expansions in momenta, that consequently become quite laborious when high-order powers of momenta are important. On the other hand, the subleading in N_c^{-1} corrections arise from one-loop meson diagrams that are well defined by the interacting piece of the bosonized NJL Lagrangian [34]. They do not involve any further parameters, and will be shown to lead to corrections to the leading order results which turn out to be large, causing on the order of a 30% reduction of the mean-field values for the polarizability coefficients.

The paper is organized as follows. A brief recollecting of the effective action for the bosonized NJL Lagrangian minimally coupled to a photon gauge field is given in Sec. II. In the original derivation [34] only the most divergent parts of quark-loop integrals are kept. This leads to an effective Lagrangian that describes a system of scalar and pseudoscalar point mesons in interaction with each other in the presence of a gauge field. However, since point particles cannot be polarized, one has to go one step further, and also include the finite parts of quark-loop integrals in an expansion of the effective action to higher orders in momentum. This is described in Sec. III.

In Sec. IV we recall the basic form of the relativistic Compton scattering amplitude and the relation to the electric and magnetic polarizability coefficients in the nonrelativistic limit. Using the effective Lagrangian approach we also confirm to $\mathcal{O}(m_\pi^2)$ the leading in N_c^{-1} results already obtained in Ref. [16].

The effective Lagrangian still contains the logarithmic and quadratic divergences of the original NJL model that appear in the coupling constant g_σ and in the gap equation for the quark mass m [34]. However, instead of solving the gap equation for m, we will rely on the sum-rule estimate [36] $m \approx \sqrt{2/3}\,\pi f_\pi$, and use the Goldberger-Treiman relation $f_\pi g_\sigma = m$ for g_σ. Then both divergences are formally accounted for in the bosonized Lagrangian in terms of the weak decay constant f_π of the Goldstone mode. Employing this Lagrangian, the subleading in N_c^{-1} contributions to the Compton amplitude are obtained in Sec. V. These contributions are given by a gauge-invariant sum of meson one-loop diagrams. Although subsets of these diagrams contain ultraviolet divergences, their sum converges, so no ultraviolet cutoff has to be introduced. In addition, individual diagrams display chiral limit divergences due to (Langacker-Pagels [37]) chiral logarithms, and the poles in m_π^2 that they contain. However, these chiral divergences *also* all cancel out in the diagram sum, and one is left with subleading amplitudes that, although nonanalytic in m_π^2, have a well-defined chiral limit. One thus obtains no-free-parameter predictions for the electric and magnetic polarizability coefficients to subleading order, that depend only on the physical observables of the pion.

The discussion of results and conclusions is presented in Sec. VI, where a comparison is made with other theoretical approaches, and experiment. Some calculational details will be found in the Appendix.

II. EFFECTIVE LAGRANGIAN

The starting point for discussing the electromagnetic polarizability of pions is taken as the bosonized version of the $U_V(1)\times \mathrm{SU}_L(2)\times \mathrm{SU}_R(2)$ invariant two-flavor Nambu–Jona-Lasinio Lagrangian that only contains pseudoscalar and scalar fields $\pi = \vec{\pi}\cdot\vec{\tau}$ and σ. In addition, the quarks are minimally coupled to an electromagnetic gauge field A_μ. Omitting details of dynamical symmetry breaking, we assume that the quarks have already been endowed with a constituent mass $m = m_0 + g_\sigma\langle\sigma\rangle$ in terms of a current quark mass m_0 and the nonvanishing expectation value of the σ field in the interacting ground state. Then, shifting to new primed fields $\sigma' = \sigma - \langle\sigma\rangle$ and $\pi' = \pi$, since $\langle\pi\rangle = 0$, one has

$$\mathcal{L}_{NJL} = \bar{\psi}[i\partial\!\!\!/ - m - g_\sigma(\sigma' + i\gamma_5\pi') - e_q A\!\!\!/)]\psi - \frac{g_\sigma^2}{4G}[\sigma'^2 + \pi'^2] - \frac{1}{4}F^2. \tag{2}$$

The meson fields in this expression thus represent fluctuations in the π and σ fields with vanishing expectation values in the chirally broken ground state of the system, and $F^2 = F_{\mu\nu}F^{\mu\nu}$ is the electromagnetic field tensor. Furthermore, $e_q = \frac{1}{2}e(\frac{1}{3} + \tau_3)$ and $g_\sigma \sim N_c^{-1/2}$ are the quark electric charge and coupling constant to the π' and σ' fields. The four component Dirac spinors ψ additionally include the N_c colors and two flavors $\tau_3 = \pm 1$ of the quark. G is a strong interaction strength parameter that must scale like N_c^{-1} in order to preserve proper QCD mass scaling.

Performing a functional integration over the quark fields in Eq. (2) now allows one to identify an equivalent action $\mathcal{A} = \int dx \mathcal{L}$ in terms of a Lagrangian $\mathcal{L} = \mathcal{L}(\sigma, \pi, A_\mu)$ that only involves meson and photon fields. The full details of

this approach were given in Refs. [34, 35]. Here we summarize only those aspects that are relevant for implementing pion polarizability calculations. One can express $\mathcal{A}$ (now dropping the primes) as

$$\mathcal{A}=\int dx\left\{-\frac{g_\sigma^2}{4G}(\sigma^2+\pi^2)+i\left\langle x\left|\mathrm{Tr}\sum_{n=2}^{\infty}\frac{1}{n}[(i\partial\!\!\!/-m)^{-1}\right.\right.\right.$$
$$\left.\left.\left.\times[g_\sigma(\sigma+i\gamma_5\pi)+e_q A\!\!\!/]]^n\right|x\right\rangle\right\}+\int dx\left\{-\frac{1}{4}F^2\right\}, \tag{3}$$

where the trace runs over all quark intrinsic indices. As shown in Ref. [34], by calculating the two-, three-, and four-point quark loop diagrams generated by the $n=\{2,3,4\}$ terms in the expansion of the fermionic determinant in Eq. (3), and then keeping only their divergent parts, one obtains an action $\mathcal{A}=\mathcal{A}_2+\mathcal{A}_3+\mathcal{A}_4+\cdots$ that involves quadratic, cubic, quartic, etc. combinations of the bosonic field amplitudes from which one identifies the Ebert-Volkov Lagrangian for the local part of a field theory of extended mesons in interaction with photons:

$$\mathcal{L}=\mathcal{L}_{free}+\mathcal{L}_{int}+\mathcal{L}_{em}+\cdots. \tag{4}$$

The noninteracting piece is

$$\mathcal{L}_{free}=\tfrac{1}{2}(\partial\pi)^2+\tfrac{1}{2}(\partial\sigma)^2-\tfrac{1}{2}m_\pi^2\pi^2-\tfrac{1}{2}m_\sigma^2\sigma^2-\tfrac{1}{4}F^2, \tag{5}$$

where $m_\pi^2=m_0 g_\sigma^2/(2mG)$ and $m_\sigma^2=4m^2+m_\pi^2$ are the pion and sigma field masses squared of the model, as generated by dynamical symmetry breaking. The meson-meson interaction terms are given by

$$\mathcal{L}_{int}=-2mg_\sigma\sigma(\sigma^2+\pi^2)-\tfrac{1}{2}g_\sigma^2(\sigma^2+\pi^2)^2. \tag{6}$$

Finally,

$$\mathcal{L}_{em}=-ie(\pi^-\partial_\mu\pi^+-\pi^+\partial_\mu\pi^-)A^\mu+e^2\pi^-\pi^+A^2 \tag{7}$$

describes the electromagnetic interaction of point pions with the gauge field.[1] Here $\mathcal{L}_{em}$ has been written in terms of pion fields carrying good isospin. The above form of $\mathcal{L}_{int}$ also exhibits the N_c dependence of the theory explicitly through the behavior $g_\sigma\sim N_c^{-1/2}$ of the coupling constant between the meson modes. In the $N_c\to\infty$ limit, the interaction term $\mathcal{L}_{int}$ falls away, and Eq. (4) reduces to a Lagrangian field theory of free point mesons interacting with photons.

III. PION STRUCTURE CORRECTIONS

A point charge cannot be polarized. Therefore, to be relevant for discussing pion polarizabilities, $\mathcal{L}$ also has to contain elements that reflect the intrinsic nonpointlike nature of a polarizable pion. A nonvanishing pion radius can arise in two ways: (i) from the intrinsic structure of the pion itself as a bound $\bar{q}q$ pair; and (ii) at higher order in N_c^{-1}, from virtual pion clouds created by $\mathcal{L}_{int}$. Technically, the inclusion of intrinsic size effects amounts to including higher-order derivatives of the pion and photon fields that accompany the finite parts of the quark loop diagrams in evaluating the action $\mathcal{A}$. We start with the finite-size contributions to an action that is quadratic in the π field. The quadratic parts in π come from the first term plus a contribution from the $n=2$ piece of the fermionic determinant in Eq. (3). One can combine these two terms as

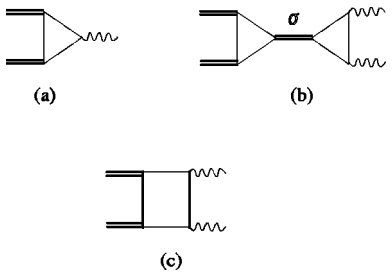

FIG. 1. Typical quark triangle and box diagrams that determine $\mathcal{L}_{\gamma\pi\pi}$ and $\mathcal{L}_{\gamma\gamma\pi\pi}$. The double and wavy lines indicate entering or exiting pions and photons. The σ propagator in (b), connecting quark triangles with photons and pions attached, generates the σ-pole contribution $\mathcal{L}^{(\sigma)}_{\gamma\gamma\pi\pi}$. The box diagram in (c) determines $\mathcal{L}^{(box)}_{\gamma\gamma\pi\pi}$.

$$\mathcal{A}_2=\frac{1}{2}g_\sigma^2\int\frac{d^4k}{(2\pi)^4}[\vec{\pi}(k)\cdot D_\pi^{-1}(k^2)\vec{\pi}(-k)] \tag{8}$$

in a momentum representation. The inverse propagator $g_\sigma^2 D_\pi^{-1}(k^2)$ for the pion is found from

$$D_\pi^{-1}(k^2)=-(2G)^{-1}+\Pi_{ps}(k^2), \tag{9}$$

where the quark one-loop pseudoscalar polarization function is given explicitly by [33]

$$\Pi_{ps}(k^2)=\frac{m-m_0}{2Gm}+g_\sigma^{-2}k^2F_\pi(k^2). \tag{10}$$

The function

$$F_\pi(q^2)=1+\frac{1}{6}q^2\langle r_\pi^2\rangle+\cdots \tag{11}$$

is identical to the leading in N_c^{-1} electromagnetic form factor of the pion as given by the simple single quark loop approximation to the $\gamma\pi\pi$ vertex shown in Fig. 1(a). The value of this vertex at low q^2 is given in Eq. (36) of Sec. IV, and allows one to identify the model (or Tarrach) radius squared [38] parameter $\langle r_\pi^2\rangle$ of the NJL Goldstone pion in this approximation as

$$\langle r_\pi^2\rangle=\frac{3}{4\pi^2 f_\pi^2}. \tag{12}$$

[1]After charge and field renormalizations [34], $e\to e(1+\frac{5}{27}e^2g_\sigma^{-2})^{1/2}$ and $A_\mu\to(1+\frac{5}{27}e^2g_\sigma^{-2})^{-1/2}A_\mu$.

Being the square of a length, this parameter combination serves as a convenient abbreviation by which to express the scattering amplitudes generated by the bosonized NJL model. The symbol f_π for the pion weak decay constant enters Eq. (12) via the Goldberger-Treiman (GT) relation $f_\pi g_\sigma = m$ that is strictly only applicable in the chiral limit $m_0 \to 0$ of vanishing current quark mass. Thus f_π (and m_π), that enter the bosonized Lagrangian, can differ in value from their measured values. We return to this point later. In the following, m will mean the value of the constituent quark mass for vanishing m_0.

Returning to the propagator $D_\pi^{-1}(k^2)$ and inserting the result given in Eq. (10) for Π_{ps}, one obtains

$$g_\sigma^2 D_\pi^{-1}(k^2) = k^2 F_\pi(k^2) - m_\pi^2 F_\pi(m_\pi^2) = (k^2 - m_\pi^2)[1 + \tfrac{1}{6}\langle r_\pi^2\rangle (k^2 + m_\pi^2)] + \cdots \tag{13}$$

after using the condition $D_\pi^{-1}(m_\pi^2) = 0$ to eliminate the quark masses and coupling constant G in terms of the pion mass. The residue of $g_\sigma^{-2} D_\pi(k^2)$ at the pion pole is thus reduced, below unity, to

$$Z = [1 + \tfrac{1}{3} m_\pi^2 \langle r_\pi^2\rangle]^{-1} \approx 1 - \tfrac{1}{3} m_\pi^2 \langle r_\pi^2\rangle. \tag{14}$$

The factor Z serves to renormalize the pion field, $\pi \to \sqrt{Z}\pi$. Carrying over this renormalization into Eq. (8), and at the same time inserting the result for $g_\sigma^2 D_\pi^{-1}(k^2)$, one obtains

$$\mathcal{A}_2 = \frac{1}{2}\int dx \left\{ (\partial\pi)^2 - m_\pi^2 \pi^2 + \frac{1}{6}\langle r_\pi^2\rangle \vec{\pi}\cdot(\partial^2 + m_\pi^2)^2 \vec{\pi} \right\} \tag{15}$$

after moving back to a coordinate representation again. Thus the noninteracting part of $\mathcal{L}$ in Eq. (5) picks up an additional term in the pion sector due to size effects that involve quartic field derivatives. These give rise to a revised Feynman propagator[2]

$$-i\Delta_\pi(k^2) = \frac{i}{(k^2 - m_\pi^2)[1 + \tfrac{1}{6}\langle r_\pi^2\rangle (k^2 - m_\pi^2)]} \tag{16}$$

for the pion mode. Both the pion field renormalization as well as the ensuing structural change in the pion propagator are essential elements of the retention of gauge invariance in the scattering amplitudes.

Turning now to the structure modifications of the electromagnetic part of the interaction with pions we isolate the $\mathcal{L}_{\gamma\pi\pi}$ and $\mathcal{L}_{\gamma\gamma\pi\pi}$ fragments of the renormalized electromagnetic Lagrangian from the $n=3$ and 4 terms in Eq. (3) that involve two pion fields and one or two photon fields, respectively. The relevant diagrams are shown in Fig. 1. For $n=3$,

$$\int dx \mathcal{L}_{\gamma\pi\pi} = i g_\sigma^2 Z \int dx \langle x | \mathrm{Tr}[(i\partial\!\!\!/ - m)^{-1} i\gamma_5 \pi (i\partial\!\!\!/ - m)^{-1} \times i\gamma_5 \pi (i\partial\!\!\!/ - m)^{-1} e_q A\!\!\!/] | x\rangle, \tag{17}$$

that involves the quark three point function of Fig. 1(a). Evaluating this up to and including cubic derivatives in the field amplitudes (combinations of second-order field derivatives cannot contribute due to the pseudoscalar and vector nature of the pion and photon, respectvely), one has

$$\begin{aligned}\mathcal{L}_{\gamma\pi\pi} = & -ieZ(\pi^-\partial_\mu\pi^+ - \pi^+\partial_\mu\pi^-)A^\mu \\ & + ie\langle r_\pi^2\rangle\{\tfrac{1}{6}(\pi^-\partial^2\partial_\mu\pi^+ - \pi^+\partial^2\partial_\mu\pi^-) \\ & - \tfrac{1}{2}(\partial_\mu\pi^-\partial^2\pi^+ - \partial_\mu\pi^+\partial^2\pi^-) \\ & + \tfrac{1}{3}(\partial_\rho\pi^-\partial^\rho\partial_\mu\pi^+ - \partial_\rho\pi^+\partial^\rho\partial_\mu\pi^-)\}A^\mu. \end{aligned} \tag{18}$$

There are two types of contributions to the effective four-point interaction Lagrangian $\mathcal{L}_{\gamma\gamma\pi\pi}$. These arise from the σ-pole and quark box diagrams depicted in Figs. 1(b) and 1(c). The σ-pole contribution is obtained by contracting the $\sigma\pi\pi$ vertex in Eq. (6) with the $\sigma\gamma\gamma$ vertex that is given by another $n=3$ fragment $\mathcal{L}_{\sigma\gamma\gamma}$ that describes a quark-loop-induced coupling of photons to the σ field. This latter vertex is determined by

$$\int dx \mathcal{L}_{\sigma\gamma\gamma} = i g_\sigma \int dx \mathrm{Tr}\langle | [(i\partial\!\!\!/ - m)^{-1}\sigma(i\partial\!\!\!/ - m)^{-1} \times e_q A\!\!\!/ (i\partial\!\!\!/ - m)^{-1} e_q A\!\!\!/] | x\rangle \tag{19}$$

or

$$\mathcal{L}_{\sigma\gamma\gamma} = \tfrac{5}{27} e^2 \langle r_\pi^2\rangle f_\pi \sigma\{(\partial_\rho A^\sigma)(\partial^\rho A_\sigma) - (\partial_\rho A^\sigma)(\partial_\sigma A^\rho)\} \tag{20}$$

after again using the abbreviation of Eq. (12) for brevity. Carrying out the contraction on the intermediate σ propagator between the two quark triangles in Fig. 1(b) then yields the separately gauge invariant contribution

$$\begin{aligned}\mathcal{L}^{(\sigma)}_{\gamma\gamma\pi\pi} &= \tfrac{1}{4}\tfrac{10}{27} e^2 \langle r_\pi^2\rangle \{(\partial_\rho A^\sigma)(\partial_\sigma A^\rho) - (\partial_\rho A^\sigma)(\partial^\rho A_\sigma)\}\pi^2 \\ &= -\tfrac{1}{4}\tfrac{5}{27} e^2 \langle r_\pi^2\rangle \pi^2 F^2, \end{aligned} \tag{21}$$

since

$$(\partial_\mu A^\nu)(\partial_\nu A^\mu) - (\partial_\mu A^\nu)(\partial^\mu A_\nu) = -\tfrac{1}{2} F^2. \tag{22}$$

The $n=4$ term in Eq. (3) includes the box diagram of Fig. 1(c). Since one is taking the trace of the fourth power of a sum of field operators, the question of operator order is important. With due regard to this aspect, one has

[2]The ghost pole in this propagator at spacelike $k^2 \sim -1$ GeV^2 is an artifact of the low momentum expansion. It plays no role in the physics.

$$\int dx\mathcal{L}^{(box)}_{\gamma\gamma\pi\pi}=\frac{i}{4}g_\sigma^2 Z\Big\{4\int dx\langle x|\mathrm{Tr}[(i\partial\!\!\!/-m)^{-1}\times e_q A\!\!\!/(i\partial\!\!\!/-m)^{-1}e_q A\!\!\!/(i\partial\!\!\!/-m)^{-1}\times i\gamma_5\pi(i\partial\!\!\!/-m)^{-1}i\gamma_5\pi]|x\rangle\Big\}+\frac{i}{4}g_\sigma^2 Z\Big\{2\int dx\langle x|\mathrm{Tr}[(i\partial\!\!\!/-m)^{-1}\times e_q A\!\!\!/(i\partial\!\!\!/-m)^{-1}i\gamma_5\pi(i\partial\!\!\!/-m)^{-1}\times e_q A\!\!\!/(i\partial\!\!\!/-m)^{-1}i\gamma_5\pi]|x\rangle\Big\}, \quad (23)$$

the factors 4 and the 2 giving the number of identical terms of each type.

Evaluation of this expression up to and including second order derivatives of the photon and pion fields in order to identify $\mathcal{L}^{(box)}_{\gamma\gamma\pi\pi}$ to that order is straightforward but cumbersome. After some calculation, one finds that there is no resultant interaction at all in the neutral channel,

$$\mathcal{L}_{\gamma\gamma\pi\pi}=\mathcal{L}^{(box)}_{\gamma\gamma\pi^0\pi^0}+\mathcal{L}^{(\sigma)}_{\gamma\gamma\pi^0\pi^0}=0, \quad (24)$$

in agreement with the (tree–level) result established previously in CHPT [11], while in the charged channel the result is

$$\begin{aligned}\mathcal{L}_{\gamma\gamma\pi\pi}&=\mathcal{L}^{(box)}_{\gamma\gamma\pi^-\pi^+}+\mathcal{L}^{(\sigma)}_{\gamma\gamma\pi^-\pi^+}\\&=e^2[Z\pi^-\pi^+-\tfrac{1}{6}\langle r_\pi^2\rangle[\pi^-\partial^2\pi^+ +\pi^+\partial^2\pi^-]]A^2\\&\quad+\tfrac{1}{4}e^2\langle r_\pi^2\rangle\{[\tfrac{8}{3}(\partial_\mu\pi^-)(\partial_\nu\pi^+)A^\mu A^\nu\\&\quad-\pi^-\pi^+[\tfrac{4}{3}A^\mu\partial^2 A_\mu+\tfrac{2}{3}(\partial_\mu A^\mu)^2]]\\&\quad+\tfrac{2}{3}\pi^-\pi^+[(\partial_\mu A^\nu)(\partial_\nu A^\mu)-\partial_\mu A^\nu)(\partial^\mu A_\nu)]\}. \quad (25)\end{aligned}$$

For real photons and pions this expression is equivalent to

$$\begin{aligned}\mathcal{L}_{\gamma\gamma\pi\pi}&=e^2\pi^-\pi^+A^2+\tfrac{2}{3}e^2\langle r_\pi^2\rangle(\partial_\mu\pi^-)(\partial_\nu\pi^+)A^\mu A^\nu\\&\quad-\tfrac{1}{12}e^2\langle r_\pi^2\rangle\pi^-\pi^+F^2, \quad (26)\end{aligned}$$

after introducing the explicit form of the pion field renormalization Z. This restores the contact term to its correct value. The term involving pion field derivatives ensures the gauge invariance of the scattering amplitudes but does not otherwise contribute to the pion polarizability. This is determined solely by the last term. Since this term involves the electromagnetic field strengths in the gauge-invariant combination $-\frac{1}{2}F^2=E^2-B^2$, the $\alpha_\pi=-\beta_\pi$ degeneracy characteristic of chiral invariance [1] will be maintained by this interaction Lagrangian.

The electromagnetic interaction $\mathcal{L}_{em}$ in Eq. (7) that includes pion structure contributions is thus upgraded to read

$$\mathcal{L}_{em}=\mathcal{L}_{\gamma\pi\pi}+\mathcal{L}_{\gamma\gamma\pi\pi}. \quad (27)$$

With this upgrade, the Ebert-Volkov Lagrangian in Eq. (4) is taken as the starting point for the polarizability calculations reported on here.

IV. COMPTON SCATTERING BY PIONS

The Compton scattering amplitude may be written as

$$f_C=-\frac{\epsilon_1^\mu W_{\mu\nu}\epsilon_2^\nu}{2\sqrt{s}} \quad (28)$$

if the photons and pions are described by plane waves of unit amplitude. The tensor $W_{\mu\nu}$ consists of a (Thompson) scattering amplitude off the total charge, plus a contribution that arises from the intrinsic structure of the target [13]:

$$W_{\mu\nu}=W^{point}_{\mu\nu}+W^{structure}_{\mu\nu}=-2e^2T^{point}_{\mu\nu}-[f_1T^{(1)}_{\mu\nu}+f_2T^{(2)}_{\mu\nu}]. \quad (29)$$

The amplitudes $f_1=f_1(s,t)$ and $f_2=f_2(s,t)$ are functions of the invariants $s=(k_1+q_1)^2=(k_2+q_2)^2$ and $t=(k_2-k_1)^2=(q_1-q_2)^2$. The three tensor coefficients in Eq. (29) have been explicitly constructed out of combinations of the pion and photon four-momenta in Ref. [13] to ensure gauge invariance separately for both the point charge and structure contributions. We will only require the explicit form of

$$T^{(2)}_{\mu\nu}=g_{\mu\nu}(q_1\cdot q_2)-q_{2\mu}q_{1\nu}, \quad (30)$$

plus the relations

$$\begin{aligned}&\epsilon_1^\mu T^{point}_{\mu\nu}\epsilon_2^\nu\to-(\vec{\epsilon}_1\cdot\vec{\epsilon}_2),\\&\epsilon_1^\mu T^{(1)}_{\mu\nu}\epsilon_2^\nu\to-(\vec{\epsilon}_1\cdot\vec{\epsilon}_2)(\omega_1\omega_2),\\&\epsilon_1^\mu T^{(2)}_{\mu\nu}\epsilon_2^\nu\to-(\vec{\epsilon}_1\cdot\vec{\epsilon}_2)(\omega_1\omega_2)+(\vec{\epsilon}_1\times\vec{q}_1)\cdot(\vec{\epsilon}_2\times\vec{q}_2)\end{aligned} \quad (31)$$

that hold near thresholds $s\to M_\pi^2$ and $t\to 0$. Then

$$\epsilon_1^\mu W_{\mu\nu}\epsilon_2^\nu\approx 2e^2(\vec{\epsilon}_1\cdot\vec{\epsilon}_2)\delta_{T_3,\pm1}-\{(\vec{\epsilon}_1\cdot\vec{\epsilon}_2)\omega_1\omega_2[f_1-f_2]+(\vec{\epsilon}_1\times\vec{q}_1)\cdot(\vec{\epsilon}_2\times\vec{q}_2)f_2]\} \quad (32)$$

in the transverse gauge. This leads to f_C in Eq. (1), with

$$\alpha_\pi=\frac{[f_1-f_2]}{2M_\pi},\quad \beta_\pi=\frac{f_2}{2M_\pi},\quad \alpha_\pi+\beta_\pi=\frac{f_1}{2M_\pi}, \quad (33)$$

after division by $-2\sqrt{s}\to-2\sqrt{M_\pi^2}$.

We very briefly retrieve some previously known leading in N_c^{-1} results using the bosonized Lagrangian, before taking up the main task of subleading corrections. The Compton scattering amplitude for charged point pions is given at tree level by the sum of contact (seagull) and pion pole diagrams [39]. Let us regenerate these contributions using the upgraded version of $\mathcal{L}_{em}$ in Eq. (27), that includes a finite pion size.

We label the contribution to the scattering tensor from $\mathcal{L}_{\gamma\gamma\pi\pi}$ in Eq. (25) as the quark box plus σ-pole contribution. This term reduces to the standard seagull diagram in the point charge limit. One has

$$W_{\mu\nu}^{(box+\sigma)}(k_1,k_2) = -2e^2[Z+\tfrac{1}{3}m_\pi^2\langle r_\pi^2\rangle]g_{\mu\nu} - \tfrac{1}{3}e^2\langle r_\pi^2\rangle\{(q_1^2+q_2^2)g_{\mu\nu}-q_{1\mu}q_{2\nu} + 2[k_{2\mu}k_{1\nu}+k_{2\nu}k_{1\mu}]\} + \tfrac{1}{3}e^2\langle r_\pi^2\rangle \times[(q_1\cdot q_2)g_{\mu\nu}-q_{2\mu}q_{1\nu}]. \quad (34)$$

The contribution from the π-pole diagram plus its crossed counterpart with the incoming and outgoing photons interchanged is

$$W_{\mu\nu}^{(\pi)}(k_1,k_2) = -\{\Gamma_\mu^{\gamma\pi\pi}(k_1,k_1+q_1)\Delta_\pi(k_2+q_2) \times\Gamma_\nu^{\gamma\pi\pi}(k_2,k_2+q_2)+\Gamma_\mu^{\gamma\pi\pi}(k_2,k_2-q_1) \times\Delta_\pi(k_2-q_1)\Gamma_\nu^{\gamma\pi\pi}(k_1,k_1-q_2)\}, \quad (35)$$

where the $\Gamma_\mu^{\gamma\pi\pi}(k_1,k_2)$ vertex is generated by $\mathcal{L}_{\gamma\pi\pi}$ of Eq. (18). This vertex is given by

$$\Gamma_\mu^{\gamma\pi\pi}(k_1,k_2) = eZ(k_1+k_2)_\mu + e\langle r_\pi^2\rangle\{\tfrac{1}{3}k_{1\mu}k_2^2+\tfrac{1}{3}k_{2\mu}k_1^2 + \tfrac{1}{6}q^2(k_1+k_2)_\mu\} \quad (36)$$

for the incoming photon four-momentum squared: $q^2=(k_1-k_2)^2$. The sum of $W_{\mu\nu}^{(box+\sigma)}$ and $W_{\mu\nu}^{(\pi)}$ is gauge invariant.

The on-shell version of $\Gamma_\mu^{\gamma\pi\pi}(k_1,k_2)$ with $k_1^2=k_2^2=m_\pi^2$ determines the electromagnetic form factor of the charged pion from

$$\Gamma_\mu^{\gamma\pi\pi}(k_1,k_2) = eF_\pi(q^2)(k_1+k_2)_\mu \quad (37)$$

to be

$$F_\pi(q^2) = Z+\tfrac{1}{3}m_\pi^2\langle r_\pi^2\rangle+\tfrac{1}{6}q^2\langle r_\pi^2\rangle = 1+\tfrac{1}{6}q^2\langle r_\pi^2\rangle \quad (38)$$

at small q^2. This was already used in Eq. (11). The pion field renormalization ensures that the $\gamma\pi\pi$ vertex carries the correct total charge, $F_\pi(0)=1$.

Contracting on the photon polarization vectors in the transverse gauge again, one finds that $\epsilon_1^\mu W_{\mu\nu}^{(\pi)}\epsilon_2^\nu$ vanishes near threshold, so that the Compton scattering in the charged channel is fully determined by the quark box plus σ-pole amplitude alone:

$$\epsilon_1^\mu W_{\mu\nu}^{(box+\sigma)}\epsilon_2^\nu = 2e^2[Z+\tfrac{1}{3}m_\pi^2\langle r_\pi^2\rangle](\vec{\epsilon}_1\cdot\vec{\epsilon}_2) + \tfrac{1}{3}e^2\langle r_\pi^2\rangle(\epsilon_1^\mu T_{\mu\nu}^{(2)}\epsilon_2^\nu). \quad (39)$$

The first term gives the correct point charge scattering since the coefficient of $2e^2$ is actually unity because of Eq. (14). The second term identifies the leading in N_c^{-1} values of the amplitudes f_1 and f_2 for charged pions as

$$f_{1\chi}^{\pm}=0, \quad f_{2\chi}^{\pm} = -\frac{1}{3}e^2\langle r_\pi^2\rangle = -\frac{\alpha}{4\pi^2 f_\pi^2}. \quad (40)$$

This value of $f_{2\chi}^{\pm}$ sets the overall model–independent scale for the pion Compton scattering amplitudes. The same scale factor appears in CHPT [22,23]. There is no scattering at all in the neutral channel at this order of approximation, $f_{1\chi}^0 = f_{2\chi}^0 = 0$. All of these amplitudes are independent of the pion mass, and thus describe the scattering in the chiral limit, $m_\pi^2\to 0$; hence the subscripts χ. Furthermore, a vanishing f_1 indicates that the chiral condition $\alpha_\pi+\beta_\pi=0$ is also satisfied. Hence

$$\alpha_{\pi\chi}^{\pm} = -\beta_{\pi\chi}^{\pm} = \frac{\alpha}{8\pi^2 m_\pi f_\pi^2}, \quad \alpha_{\pi\chi}^0 = -\beta_{\pi\chi}^0 = 0, \quad (41)$$

with $M_\pi\to m_\pi$, the pion mass of the model. We refer to these values as the polarizability coefficients of a chiral (Goldstone) pion.

The degeneracy in the magnitude of the chiral electric and magnetic polarizabilities is lifted in the next order of approximation when higher-order momentum contributions are considered in $\mathcal{L}_{\gamma\gamma\pi\pi}$. This involves expanding the σ-pole and quark box diagrams in Fig. 1 to $\mathcal{O}(p^6)$. Omitting the details, one finds that

$$f_1^0 = \frac{1}{3}e^2\langle r_\pi^2\rangle\left(\frac{5}{9}\frac{m_\pi^2}{m^2}\right),$$

$$f_2^0 = -\frac{1}{3}e^2\langle r_\pi^2\rangle\left(\frac{5}{9}m_\pi^2\langle r_\pi^2\rangle-\frac{5}{6}\frac{m_\pi^2}{m^2}\right) \quad (42)$$

and

$$f_1^{\pm} = \frac{1}{3}e^2\langle r_\pi^2\rangle\left(\frac{7}{45}\frac{m_\pi^2}{m^2}\right),$$

$$f_2^{\pm} = -\frac{1}{3}e^2\langle r_\pi^2\rangle\left(1+\frac{5}{9}m_\pi^2\langle r_\pi^2\rangle-\frac{1}{3}\frac{m_\pi^2}{m^2}\right) \quad (43a)$$

for the neutral and charged channels, respectively. As before, the tacit assumption has been made that the GT relation $f_\pi g_\sigma = m$ is unaltered by the presence of a current quark mass in the NJL gap equation. This is not strictly true once $\mathcal{O}(m_\pi^2)$ contributions are included. Considering a finite current quark mass changes [40] the values of $m^2\to\tilde{m}^2$, $g_\sigma^{-2}\to\tilde{g}_\sigma^{-2}$ that causes these scattering amplitudes to be multiplied by a global factor $Zf_\pi^2\tilde{g}_\sigma^2/\tilde{m}^2\approx 1+\tfrac{1}{6}m_\pi^2\langle r_\pi^2\rangle-\tfrac{1}{2}m_\pi^2/m^2$. To order $\mathcal{O}(m_\pi^2)$, this only affects the amplitude $f_2^{\pm}$ because of the $\mathcal{O}(p^4)$ tree level term it contains. It is replaced by

$$f_2^{\pm}\to\tilde{f}_2^{\pm}\approx -\frac{1}{3}e^2\langle r_\pi^2\rangle\left(1+\frac{13}{18}m_\pi^2\langle r_\pi^2\rangle-\frac{5}{6}\frac{m_\pi^2}{m^2}\right). \quad (43b)$$

These expressions correspond exactly to keeping at most $\mathcal{O}(p^6)$ contributions in external momenta in terms of the

classification scheme adopted in Ref. [16]. The amplitudes f_2 tend to a finite constant or vanish respectively in the charged or neutral channel as $m_\pi^2 \to 0$; f_1 vanishes in both channels. The null values[3] for f_1^0 and f_2^0 as $m_\pi^2 \to 0$ just reflect the pointlike nature of the neutral Goldstone pion of zero charge radius in the chiral limit [12]. Such a point object cannot be polarized. Here this result comes about as a consequence of an exact cancellation between the scattering amplitudes arising from the quark box and σ-pole diagrams in this limit.

The associated leading in N_c^{-1} polarizabilities can be read off to $\mathcal{O}(m_\pi^2)$ from Eqs. (33). Note, however, that the pion mass $M_\pi \approx m_\pi(1+\frac{1}{6}m_\pi^2\langle r_\pi^2\rangle - m_\pi^2/8m^2)$ that enters into that equation also differs from m_π by $\mathcal{O}(m_\pi^2)$ nonchiral corrections [40]. Then

$$\alpha_\pi^0 + \beta_\pi^0 = \frac{\alpha}{8\pi^2 m_\pi f_\pi^2}\left(\frac{5}{9}\frac{m_\pi^2}{m^2}\right), \tag{44a}$$

$$\beta_\pi^0 = -\frac{\alpha}{8\pi^2 m_\pi f_\pi^2}\left(\frac{5m_\pi^2}{12\pi^2 f_\pi^2} - \frac{5}{6}\frac{m_\pi^2}{m^2}\right) \tag{44b}$$

for π^0, and

$$\alpha_\pi^\pm + \beta_\pi^\pm = \frac{\alpha}{8\pi^2 m_\pi f_\pi^2}\left(\frac{7}{45}\frac{m_\pi^2}{m^2}\right), \tag{45a}$$

$$\beta_\pi^\pm = -\frac{\alpha}{8\pi^2 m_\pi f_\pi^2}\left(1 + \frac{5m_\pi^2}{12\pi^2 f_\pi^2} - \frac{17}{24}\frac{m_\pi^2}{m^2}\right) \tag{45b}$$

for $\pi^\pm$, after making the replacement $f_2^\pm \to \tilde{f}_2^\pm$ for calculating $\beta_\pi^\pm$. These results are identical up to $\mathcal{O}(m_\pi^2)$ with the exact leading in N_c^{-1} computations in Ref. [16] for the NJL model electric and magnetic polarizability coefficients, after letting their cutoff $\Lambda \to \infty$. If in addition the quark mass m is taken equal to its sum rule value [36], this set of equations makes predictions for these coefficients that only involve the known physical constants of the pion. Using $m_\pi = 140.2$ MeV and $f_\pi = 88.8$ MeV as appropriate NJL model input values (see Sec. VI) after inserting $m \approx \sqrt{2/3}\pi f_\pi \approx 228$ MeV, one has, in units of 10^{-4} fm^3,

$$\alpha_\pi^\pm = \frac{\alpha}{8\pi^2 m_\pi f_\pi^2}\left(1 - \frac{33m_\pi^2}{80\pi^2 f_\pi^2}\right) \approx 5.75 \ \ [4.98],$$

$$\beta_\pi^\pm = -\frac{\alpha}{8\pi^2 m_\pi f_\pi^2}\left(1 - \frac{31m_\pi^2}{48\pi^2 f_\pi^2}\right) \approx -5.37 \ \ [-4.57], \tag{46}$$

$$\alpha_\pi^0 = 0 \ \ [-0.09],$$

$$\beta_\pi^0 = \frac{\alpha}{8\pi^2 m_\pi f_\pi^2}\left(\frac{5m_\pi^2}{6\pi^2 f_\pi^2}\right) \approx 1.35 \ \ [1.54].$$

Note that $\alpha_\pi^\pm \approx -\beta_\pi^\pm$ come to within 80–90 % of their common chiral value $\alpha_{\pi\chi}^\pm \approx 6.42$ in Eq. (41), while $\alpha_\pi^0 = 0$ returns to its chiral value. Only β_π^0 has been changed appreciably by $\mathcal{O}(m_\pi^2)$ contributions. Actually solving the gap equation for reasonable input parameters places [33] m in the range $\sim$200–240 MeV that does not differ substantially from the corresponding sum-rule estimate for m given above. Consequently to $\mathcal{O}(m_\pi^2)$, the values of the leading order electric and magnetic polarizabilities will still mainly be determined by the chiral properties of the Goldstone pion.

These leading-order estimates differ somewhat from the corresponding $\mathcal{O}(p^4+p^6)$ values given in Ref. [16] (shown in square brackets) because of our slightly different choice of the effective f_π, m_π, and m, but more especially because their (convergent) integrals that determine the polarizability are cut off with the same $\Lambda \sim 1$ GeV that is necessary for an actual calculation of m. In the present approach this would correspond to introducing an additional parameter Λ^2/m^2 by cutting off all quark loop integrals, convergent or not, that determine the structure of the interaction Lagrangian.

V. SUBLEADING IN N_C^{-1} CORRECTIONS

We next set up the main task of identifying and computing the subleading in N_c^{-1} corrections due to meson-meson interaction terms described by $\mathcal{L}_{int}$ in Eq. (6). Intermediate meson loops are introduced by this interaction, that generate meson clouds which make a contribution of their own to the pion charge radius.

The set of direct Compton scattering diagrams that are subleading is shown in Fig. 2. Not shown are the crossed diagrams with the initial and final photon states interchanged, that must accompany each direct diagram. Neither are the three ''seagull'' diagrams shown that match Figs. 2(c)–2(e) in structure, but have the two photons attached at a common point instead of sequentially. The complete set, direct plus crossed, plus matching seagull diagrams, generate the subleading $O(N_c^{-1})$ Compton scattering amplitude contribution that is gauge invariant. Since these contributions are all subleading, we may use the point-charge form given by Eq. (7) to describe the photon-pion interactions for this stage of the calculation. The introduction of the transverse gauge for the photon polarization after moving to the long-wave limit results in an essential simplification at this point. For then only the subset of diagrams (c), (d), and (e) of Fig. 2 need to be considered, since only these will survive contraction with the transverse polarization vectors.

[3] As an aside we point out that the vanishing of the neutral amplitudes in the chiral limit can also be understood in terms of Dashen's theorem. This theorem [41] shows that a neutral Goldstone pion remains a Goldstone pion (i.e., cannot develop electromagnetic mass) in the presence of electromagnetic interactions as a consequence of chiral symmetry. The electromagnetic self-mass squared can be obtained [42] from the Compton scattering tensor by simply contracting the photon lines in Figs. 1(b) and 1(c). A vanishing scattering amplitude in the neutral channel is thus sufficient (but not necessary; see Sec. V B) to make the electromagnetic self-energy also vanish in the chiral limit, in line with this theorem.

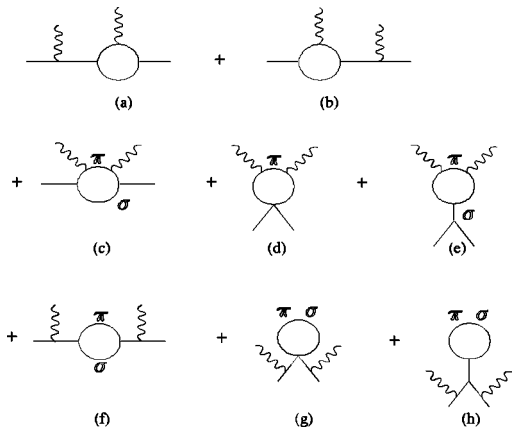

FIG. 2. The complete set of Compton scattering diagrams that are subleading in N_c^{-1}. Wavy lines indicate photons, and solid lines indicate mesons. Only direct diagrams are drawn. To these must be added another eight diagrams with incoming and outgoing photons interchanged, plus a further three seagull diagrams that match (c), (d), and (e) in structure, but with the photons attached at a common point instead of sequentially.

A. Neutral channel

In the neutral channel charge conservation removes Fig. 2(c) from consideration too, so only Figs. 2(d) and 2(e) are relevant. Since the pion in the loop must be charged in order to couple to a photon, the four-pion vertex for Fig. 2(d) only involves that piece of the four-pion interaction Lagrangian in Eq. (6) where at least two of the pion fields are charged. On the other hand, the two vertices at the ends of the σ meson propagator in Fig. 2(e) are determined by the $\mathcal{L}_{\sigma\pi\pi} = -2mg_\sigma \sigma\pi^2$ term in $\mathcal{L}_{int}$. With the eventual limit $t\to 0$ in mind, it becomes convenient to generate the diagram sum of Figs. 2(d) and 2(e) from a common interaction Lagrangian by contracting the σ meson line, and adding the result to the four-pion Lagrangian with due regard to differing symmetry factors for charged and neutral channels. Then

$$\mathcal{L}^{(2d+2e)}_{\pi\pi\pi\pi} = -\frac{1}{2}g_\sigma^2\left\{4\frac{m_\pi^2}{m_\sigma^2}[\pi^0\pi^0\pi^-\pi^+] + \frac{1}{2}\left(1+\frac{m_\pi^2}{m_\sigma^2}\right)[4\pi^-\pi^+\pi^-\pi^+]\right\} \quad (47)$$

where the relation $m_\sigma^2 = 4m^2 + m_\pi^2$ has been used.

The first term in Eq. (47) determines the scattering contribution in the neutral channel. Upon coupling two photons to the charged pion loop, either via a photon seagull or sequentially, one finds that both loops diverge logarithmically, but that their sum is finite. The tensor scattering amplitude is given by

$$W^{(2d+2e)}_{\mu\nu}(q_1,q_2) = -8ie^2g_\sigma^2\frac{m_\pi^2}{m_\sigma^2}\{g_{\mu\nu}I(m_\pi^2,m_\pi^2;t) - J_{\mu\nu}(q_1,q_2)\}, \quad (48)$$

where $t=(q_1-q_2)^2$. The integrals I and $J_{\mu\nu}$, which are individually divergent, are defined in Eqs. (A1) and (A3). They determine the contributions of the seagull and sequentially scattered photons, respectively. However, the difference $[g_{\mu\nu}I(m_\pi^2,m_\pi^2;t) - J_{\mu\nu}(q_1,q_2)]$ is convergent, and behaves like $\sim 1/m_\pi^2$ for on-shell photons as $t\to 0$. Thus the scattering amplitude $W^{(2d+2e)}_{\mu\nu}$ becomes independent of the pion mass, and consequently *finite* in the chiral limit.

We contract with the photon polarization vectors as before, to find

$$\epsilon_1^\mu W^{(2d+2e)}_{\mu\nu}\epsilon_2^\nu = -\frac{1}{3(1+y)}\frac{e^2}{(4\pi)^2 f_\pi^2}(\epsilon_1^\mu T^{(2)}_{\mu\nu}\epsilon_2^\nu), \quad (49)$$

after again employing the GT relation $f_\pi g_\sigma = m$ and the abbreviations $y = m_\pi^2/\mu^2$ with $\mu = 2m$. It then follows that the subleading in N_c^{-1} corrections to f_1 and f_2 in the neutral channel are

$$\delta f_1^0 = 0, \quad \delta f_2^0 = \frac{1}{36}e^2\langle r_\pi^2\rangle\frac{1}{(1+y)}. \quad (50)$$

Thus f_1^0 is unchanged from its leading value, while f_2^0 is replaced by

$$f_2^0 + \delta f_2^0 = -\frac{1}{3}e^2\langle r_\pi^2\rangle\left(\frac{5}{9}m_\pi^2\langle r_\pi^2\rangle - \frac{13}{4}\frac{m_\pi^2}{\mu^2} - \frac{1}{12}\right), \quad (51)$$

after only keeping subleading corrections to $\mathcal{O}(m_\pi^2)$ for consistency.

Since the sum $f_2^0 + \delta f_2^0$ no longer vanishes in the chiral limit, the question arises of what has become of Dashen's theorem. However, this theorem concerns itself solely with the vanishing electromagnetic mass correction of the chiral π^0, not its polarizability, and continues to hold. This is seen as follows. The electromagnetic (EM) mass shift squared, $\delta m^2_{\pi^0}$, due to these meson loops is again found by contracting on the photons in the Compton tensor amplitudes in Fig. 2 (and dividing by 2 to compensate for crossing). This introduces the photon propagator $-iD_{\mu\nu}(q^2) = -ig_{\mu\nu}/q^2$. The gauge choice is immaterial, since $\delta m^2_{\pi^0}$ is explicitly gauge invariant. Then

$$\delta m^2_{\pi^0} = \frac{1}{2}\int\frac{d^4q}{(2\pi)^4}[-iD^{\mu\nu}(q^2)]W^{(2d+2e)}_{\mu\nu}(q,q) \sim e^2m_\pi^2\left(\frac{\Lambda^2}{m_\sigma^2}\right)\left\{1+\frac{1}{3}\ln\frac{m_\pi^2}{\Lambda^2}+\cdots\right\}, \quad (52)$$

with the help of Eq. (48), after regulating the divergent integral with a sharp cutoff Λ in Euclidean momentum space. Thus the $\mathcal{O}(N_c^{-1})$ EM mass correction continues to vanish in the chiral limit.

B. Charged channel

The contributions of Figs. 2(d) and 2(e) in the charged channel follow from the last term of Eq. (47). This gives rise to the same expression as Eq. (48), but with m_π^2/m_σ^2 replaced by $1+m_\pi^2/m_\sigma^2$. One now has

$$W_{\mu\nu}^{(2d+2e)\pm}=-\frac{e^2}{(4\pi)^2 f_\pi^2}\left(\frac{1}{3y}+\frac{1}{3(1+y)}\right)T_{\mu\nu}^{(2)}. \quad (53)$$

This amplitude develops a chiral pole at $y\to 0$. The remaining contribution in the charged channel is given by Fig. 2(c). Translating the diagram, one finds that

$$W_{\mu\nu}^{(2c)\pm}=-8ie^2g_\sigma^2(4m^2)\{g_{\mu\nu}J(k_1,k_2)-\tfrac{1}{2}I_{\mu\nu}(q_1,k_1,k_2) -\tfrac{1}{2}I_{\nu\mu}(-q_2,k_1,k_2)\}. \quad (54)$$

The integrals $J(k_1,k_2)$ and $I_{\mu\nu}(q_1,k_1,k_2)$ are given in Eqs. (A5) and (A6). We require their $t\to 0$ limit after contraction with the polarization vectors. Although $J(k_1,k_2)$ and $I_{\mu\nu}(q_1,k_1,k_2)$ individually display chiral singularities $\sim\ln y$ and $\sim 1/y$, the logarithmic terms cancel out in the combination required in Eq. (54). Using the $y\to 0$ limiting forms for these integrals, one obtains

$$\epsilon_1^\mu W_{\mu\nu}^{(2c)\pm}\epsilon_2^\nu=2e^2\left(\frac{g_\sigma^2}{8\pi^2}\right)\left\{1+\frac{8}{3}y+2y\ln y+\cdots\right\}(\vec{\epsilon}_1\cdot\vec{\epsilon}_2) -\frac{e^2}{(4\pi)^2 f_\pi^2}\left\{-\frac{1}{3y}+1+\frac{119}{18}y+\frac{10}{3}y\ln y +\cdots\right\}(\epsilon_1^\mu T_{\mu\nu}^{(2)}\epsilon_2^\nu). \quad (55)$$

The remaining simple pole in this expression is in turn canceled by an identical pole in $W_{\mu\nu}^{(2d+2e)\pm}$. Consequently the final scattering correction to $\mathcal{O}(m_\pi^2)$ and $\mathcal{O}(m_\pi^2\ln m_\pi^2)$ in the charged channel is given by

$$\epsilon_1^\mu W_{\mu\nu}^{(2c+2d+2e)\pm}\epsilon_2^\nu =2e^2\left(\frac{g_\sigma^2}{8\pi^2}\right)\left\{1+\frac{8}{3}y+2y\ln y+\cdots\right\}(\vec{\epsilon}_1\cdot\vec{\epsilon}_2) -\frac{e^2}{(4\pi)^2 f_\pi^2}\left\{\frac{4}{3}+\frac{113}{18}y+\frac{10}{3}y\ln y+\cdots\right\}(\epsilon_1^\mu T_{\mu\nu}^{(2)}\epsilon_2^\nu), \quad (56)$$

that is nonanalytic in $y=m_\pi^2/\mu^2$ but free of all chiral divergences. The subleading scattering amplitude corrections are thus

$$\delta f_1^\pm=0, \quad \delta f_2^\pm=\frac{1}{3}e^2\langle r_\pi^2\rangle\left(\frac{1}{3}+\frac{113}{72}y+\frac{5}{6}y\ln y+\cdots\right). \quad (57)$$

There is again no correction to $f_1^\pm$. However, there is now a spurious correction to the point charge scattering, coming from the first term $\sim(\vec{\epsilon}_1\cdot\vec{\epsilon}_2)$ in Eq. (56) which is unphysical. This is in turn removed by subleading $\mathcal{O}(N_c^{-1})$ corrections to the pion field renormalization. One sees this by calculating the correction $-i\delta\Sigma(k^2)=ig_\sigma^2\delta\Pi_{ps}(k^2)$ to the pion self-energy. This is given by the sum of diagrams 2(f) plus 2(g) plus 2(h) of the last row in Fig. 2 with the photons removed. With the help of $\mathcal{L}_{int}$ in Eq. (6), one finds that the $k^2=0$ value of Fig. 2(f) just cancels out against the k^2–independent contribution from the sum of Figs. 2(g) and 2(h). Then

$$\delta\Pi_{ps}(k^2)=-16im^2\{I(m_\sigma^2,m_\pi^2;k^2)-I(m_\sigma^2,m_\pi^2;0)\} \approx\frac{k^2}{8\pi^2}, \quad k^2\to 0. \quad (58)$$

The integral $I(m_\sigma^2,m_\pi^2;k^2)$ is given by Eq. (A1). The difference vanishes like k^2, confirming that the Goldstone nature of the chiral pion is strictly preserved. We replace the pseudoscalar polarization $\Pi_{ps}(k^2)$ in Eq. (9) by the sum $\Pi_{ps}(k^2)+\delta\Pi_{ps}(k^2)$, and find that the residue at the pole $k^2=m_\pi^2$ of the modified pion propagator is altered from Z to Z', where

$$Z'=\left[1+\frac{1}{3}m_\pi^2\langle r_\pi^2\rangle+g_\sigma^2\left(\frac{\partial}{\partial k^2}\delta\Pi_{ps}\right)_{m_\pi^2}\right]^{-1} \approx 1-\frac{1}{3}m_\pi^2\langle r_\pi^2\rangle-\frac{g_\sigma^2}{8\pi^2}\left(1+\frac{8}{3}y+2y\ln y+\cdots\right) \quad (59)$$

after appealing to Eq. (A2). The correct point-charge scattering is restored by replacing Z with Z' in the point scattering term $\sim(\vec{\epsilon}_1\cdot\vec{\epsilon}_2)$ in Eq. (39), and adding this to the corresponding point scattering contribution that appears in Eq. (56).

VI. RESULTS AND CONCLUSIONS

We have seen that the subleading in N_c^{-1} corrections to the Compton scattering tensor appear in the amplitude f_2 but not f_1 in either channel. Thus these corrections influence the electric and magnetic polarizability coefficients individually, but not the leading in N_c^{-1} values of their sums which are immune to the class of subleading corrections considered here. This finding is also in line with the results of CHPT [9]. To quantify the changes in the individual coefficients we start with the magnetic polarizability and write

$$\beta_\pi^{T_3}=-\frac{\alpha}{8\pi^2 m_\pi f_\pi^2}\chi^{T_3}(x,y), \quad x=m_\pi^2/f_\pi^2, \ y=m_\pi^2/\mu^2, \quad (60)$$

where T_3 is the third component of the channel isospin. Then

TABLE I. Breakdown into leading and subleading in N_c^{-1} contributions to the charged pion polarizability coefficients for the bosonized NJL model. The input parameters are $m_\pi = 140.2$ MeV and $f_\pi = 88.8$ MeV at a quark mass of $m = 227.8$ MeV, as given by the sum rule, so that $\mu = m_\sigma \approx 0.46$ GeV. These parameters reproduce the observed values of $F_\pi \approx 93$ MeV for the weak decay constant and an average meson mass of $M_\pi \approx 138$ MeV. For a critical overview of data extraction, see Refs. [7,9,22]. Units are 10^{-4} fm^3.

	$\alpha_\pi^\pm + \beta_\pi^\pm$	$\alpha_\pi^\pm - \beta_\pi^\pm$	$\alpha_\pi^\pm$	$\beta_\pi^\pm$
Leading	0.38	11.13	5.75	-5.37
Subleading	0	-3.80	-1.90	1.90
Total	0.38	7.33	3.85	-3.47
Expt.	$0.22 \pm 0.07(\text{stat.}) \pm 0.04(\text{sys.})$ [5,7]			
	$0.33 \pm 0.06 \pm 0.01$ [6,7]			
	$1.4 \pm 3.1 \pm 2.5$ [4]			
		4.8 ± 1.0 [5,7]	2.5 ± 0.5	-2.3 ± 0.5
		6.03 ± 1.26 [5]		
		$15.6 \pm 6.4 \pm 4.4$ [4]	8.5 ± 6.1	-7.1 ± 6.1
		17.09 ± 3.5 [3]		

$$\chi^0(x,y) = \left[\left(\frac{5}{12\pi^2} x - \frac{10}{3} y + \cdots \right) + \left(-\frac{1}{12} + \frac{1}{12} y + \cdots \right) \right] \tag{61}$$

and

$$\chi^\pm(x,y) = \left[\left(1 + \frac{5}{12\pi^2} x - \frac{17}{6} y + \cdots \right) - \left(\frac{1}{3} + \frac{113}{72} y + \frac{5}{6} y \ln y + \cdots \right) \right] \tag{62}$$

for the neutral and charged channels, respectively, using Eqs. (50) and (57). The leading and subleading in N_c^{-1} contributions in these expressions have been bracketed separately. Note that χ^0 and $\chi^\pm$ are reduced from zero and unity to $-1/12$ and 2/3, respectively, by the subleading contributions in the chiral limit.

Besides the order parameter f_π that sets the energy scale for chiral symmetry restoration by external influences [33], the nonchiral terms in these expressions require an additional scale parameter against which to compare m_π. For the bosonized NJL model we have seen that $\mu = 2m \approx m_\sigma$ provides such a scale in terms of the scalar field mass. This is the only place where the NJL model parameters enter into the polarizability calculations. As already remarked, we can circumvent even these by taking the sum rule value $m \approx 228$ MeV for the quark mass instead of solving for m from the gap equation that depends on the NJL coupling constant G plus a regulating cutoff Λ. This choice of m corresponds to the scale of $\mu \approx 456$ MeV. In obtaining numerical estimates we have used the ''adjusted'' values $m_\pi = 140.2$ MeV and $f_\pi = 88.8$ MeV that reproduce the observed average pion mass and decay constant at $M_\pi \approx 138$ MeV and $F_\pi \approx 93$ MeV respectively, after taking into account, as in CHPT [19], that the bare constants m_π and f_π of the model, differ by nonchiral corrections from their observed values. The relations for making these adjustments for the NJL model are given in Ref. [40].

Using these input values in Eqs. (60), (45a), and (44a), we obtain the breakdown into leading and subleading contributions given in Tables I and II. The subleading corrections have a significant effect. While the sum $\alpha_\pi + \beta_\pi$ is not affected in either channel, there is more than a 30% reduction in $\alpha_\pi - \beta_\pi$, and therefore in the values of the individual coefficients in the charged channel due to $\mathcal{O}(N_c^{-1})$ contributions. These corrections are much larger than the $\sim 6\%$ corrections of $\mathcal{O}(p^4 + p^6)$, leading in N_c^{-1} values of these coefficients due to retaining *all* orders of external momenta as reported in [16]. So neglecting $\mathcal{O}(p^8)$ and higher momentum contributions in the row labeled ''leading'' in Table I, as we have done here, will not make much difference to our final results.

The polarization coefficients in the neutral channel behave differently. Although the sum $\alpha_\pi^0 + \beta_\pi^0$ is again independent of subleading contributions, α_π^0 is determined almost totally by them, while β_π^0 is almost independent of these contributions. The reason for this is clear from the simple analytic expressions

$$\alpha_\pi^0 = \frac{\alpha}{8\pi^2 m_\pi f_\pi^2} \left(-\frac{1}{12} + \frac{m_\pi^2}{32\pi^2 f_\pi^2} \right),$$

TABLE II. A repetition of the calculations described in Table I, but for the neutral pion. Data from the Mark II and Crystal Ball Collaborations [5].

	$\alpha_\pi^0 + \beta_\pi^0$	$\alpha_\pi^0 - \beta_\pi^0$	α_π^0	β_π^0
Leading	1.35	-1.35	0	1.35
Subleading	0	-0.98	-0.49	0.49
Total	1.35	-2.33	-0.49	1.84
Expt.	1.25 ± 0.06	-1.4 ± 1	-0.08 ± 0.50	1.33 ± 0.50

TABLE III. Comparison of various estimates of the sum and difference $\alpha_\pi \pm \beta_\pi$ for charged and neutral pions.

Charged pions	$\alpha_\pi^\pm + \beta_\pi^\pm$	$\alpha_\pi^\pm - \beta_\pi^\pm$
From Table I	0.38	7.33
Bajc *et al.* [16]	0.33	10.0
CHPT, one loop [22]	0	5.4 ± 0.8
CHPT, two loops [22]	0.3 ± 0.1	4.4 ± 1.0
Dispersion sum rules [24]	0.39 ± 0.04	~ 10.8
DMO sum rule, QCD estimate of spectral densities [30]	0	11.2 ± 1.0
DMO sum rule, spectral densities on a lattice [31]	0	$-4.0 \pm 3.6 \pm 3.2$
DMO sum rule, empirical spectral densities [28,27]	0	-6.0
DMO experimental spectral densities ($s \lesssim 3$ GeV^2) [29]	0	$\sim 16 \pm 2$
DMO sum rule, NJL model spectral densities [27]	0	8.56
DMO sum rule, ENJL model spectral densities [27]	0	3.2 to 10.4
Experimental range	~ 0.22 to 1.4	~ 4.8 to 17.1
Neutral pions	$\alpha_\pi^0 + \beta_\pi^0$	$\alpha_\pi^0 - \beta_\pi^0$
From Table II	1.35	-2.33
Bajc *et al.* [16]	1.19	-2.16
CHPT, one loop [9]	0	-1.01
CHPT, two loops plus chiral logs. [9]	1.15 ± 0.30	-1.90 ± 0.20
Dispersion sum rules [24]	1.04 ± 0.07	~ 10.0
Experimental range	~ 1.25	~ -1.4

$$\beta_\pi^0 = \frac{\alpha}{8\pi^2 m_\pi f_\pi^2}\left(\frac{1}{12} + \frac{77 m_\pi^2}{96\pi^2 f_\pi^2}\right). \tag{63}$$

that follow from Eqs. (44a) and (61). These expressions, which reduce to the standard CHPT one-loop result $\alpha_\pi^0 = -\beta_\pi^0 = -\alpha/(96\pi^2 m_\pi f_\pi^2)$ for the neutral pion for $m_\pi^2 \to 0$, show that the subleading chiral contribution of $-1/12$ dominates the value of α_π^0 but is overshadowed by the nonchiral term in β_π^0. As already pointed out, for reasonable values of m the leading contribution to α_π^0 is always near zero. For the sum rule value of m used to derive Eq. (63) it is exactly zero. Consequently the final value of α_π^0 is determined almost entirely by subleading contributions. Finally we note that the disparity in $\pi^\pm$ and π^0 intrinsic polarizability values simply reflects the quasi-point-like nature of the neutral (Goldstone) pion.

The $\mathcal{O}(N_c^{-1})$ calculations of the pion polarizability reported here are contrasted in Table III with values obtained from other calculations. We have also included an inferred measurement of the polarization difference in the charged channel as deduced from the ALEPH data in conjunction with the DMO sum rule. These data seem to saturate this sum rule for $s \lesssim 3$ GeV^2, when judged against the chiral predictions [43] for it.

From Table III one sees that, except for the DMO sum rule which gives zero by construction, all the calculated values of $\alpha_\pi^\pm + \beta_\pi^\pm$ are consistent and in reasonable accord with the data. On the other hand there is a considerable spread in the values of the charged pion polarizability difference. In particular, the DMO values of $\alpha_\pi^\pm - \beta_\pi^\pm = 2\alpha_\pi^\pm$ vary between -6.0 and 11.2. This spread of values reflects the uncertainty in the DMO sum-rule estimate of the intrinsic polarizability of the charged pion, which is always negative [1], typically two orders of magnitude greater than that of the neutral pion, and consequently of a similar magnitude as the recoil [44] contribution $\alpha_{recoil}^\pm = \alpha\langle r_\pi^2\rangle/(3M_\pi) \approx 15 \times 10^{-4}$ fm^3 from which it is subtracted.

The role of vector meson excitations [8] ought to be considered too, since their inclusion also gives rise to leading order contributions to the Compton amplitude within the N_c^{-1} classification scheme. Such excitations have been mimicked in the extended NJL model [45] by including modes carrying the quantum numbers of the ρ and a_1 mesons in a chirally invariant manner. Although some results in the form of numerical fits to leading order calculations for $\gamma\gamma \to \pi^0\pi^0$ are available [15], a systematic investigation of the role of vector modes on Compton scattering within the bosonized ENJL model framework, including both leading and subleading chiral and nonchiral contributions, is still lacking. But in leading order, in the chiral limit at least, the main physical consequence of including the ρ plus a_1 chiral partner vector modes is the occurrence of $\pi - a_1$ mixing [46,45]. As discussed in Refs. [27,47] this leads to an additional induced axial vector coupling characterized by the size of the quark axial coupling constant $g_A \lesssim 1$, that shrinks the calculated pion rms radius by a factor $\sqrt{g_A}$ while at the same time rescaling [48] both $f_\pi \to f'_\pi = \sqrt{g_A} f_\pi$, and $g_\sigma \to g'_\sigma = g_\sigma/\sqrt{g_A}$. The combined effect is to reduce the Tarrach radius parameter by g_A^2, and thus to quench the chiral limit values of the electric and magnetic polarizabilities by the same factor. In combination with the DMO sum rule, this gives the ENJL model range of values for charged pions listed in Table III.

In summary, the role of subleading in N_c^{-1} meson one-loop corrections on the pions' polarizability coefficients has been investigated within the bosonized version of the minimal Nambu–Jona-Lasio model. We have shown that, while

leaving the leading order values of the polarizability sums $\alpha_\pi+\beta_\pi$ unaltered in both charged and uncharged channels in agreement with CHPT, such corrections lead to significant changes in the leading in N_c^{-1} values of the polarizability coefficients themselves in the charged channel. These conclusions are independent of any regulating cutoffs or model parameters, since the final results have been expressed entirely in terms of the physical observables of the pion.

APPENDIX: EVALUATION OF LOOP INTEGRALS

The following loop integrals are required to evaluate the subleading Feynman diagrams for Compton scattering amplitudes.

(i) The integral

$$I(m_\sigma^2,m_\pi^2;k^2)=\int\frac{d^4l}{(2\pi)^4}\frac{1}{[(l+k)^2-m_\pi^2][l^2-m_\sigma^2]}$$
$$=\frac{i}{(4\pi)^2}\int_0^1 d\alpha\int_{\{R\}}^\infty\frac{d\rho}{\rho}$$
$$\times e^{-i\rho[m_\sigma^2(1-\alpha)+m_\pi^2\alpha-k^2\alpha(1-\alpha)]}, \quad \text{(A1)}$$

together with a suitable gauge-preserving regularization prescription $\{R\}$, gives the loop integral for two-point amplitudes. However, the difference $I(m_\sigma^2,m_\pi^2;k^2)-I(m_\sigma^2,m_\pi^2;0)\sim\delta\Pi_{ps}$, which determines the subleading in N_c^{-1} correction to the pion self-energy, is convergent. The derivative of $\delta\Pi_{ps}$ at $k^2=m_\pi^2$ is required for calculating the pion propagator renormalization to $\mathcal{O}(N_c^{-1})$. In view of Eqs. (58) and (A1), this is given by

$$\frac{\partial}{\partial k^2}\delta\Pi_{ps}=\frac{m^2}{\pi^2}\int_0^1 d\alpha\frac{\alpha(1-\alpha)}{m_\sigma^2\alpha+m_\pi^2(1-\alpha)^2}$$
$$=\frac{1}{8\pi^2}\left\{1+\frac{8}{3}y+2y\ln y+\cdots\right\}, \quad \text{(A2)}$$

with $y=m_\pi^2/\mu^2$ as before.

(ii) The subleading in N_c^{-1} contribution to the neutral channel depicted in Figs. 2(d) and 2(e) is proportional to the combination $[g_{\mu\nu}I(m_\pi^2,m_\pi^2;t)-J_{\mu\nu}(q_1,q_2)]$, where

$$J_{\mu\nu}(q_1,q_2)$$
$$=\int\frac{d^4l}{(2\pi)^4}\frac{(2l-q_1)_\mu(2l-q_2)_\nu}{[(l-q_1)^2-m_\pi^2][l^2-m_\pi^2][(l-q_2)^2-m_\pi^2]}. \quad \text{(A3)}$$

Note that the ''crossed'' version of $J_{\mu\nu}(q_1,q_2)$ with $q_1\to-q_2$, $\mu\to\nu$ is identical to itself. This integral diverges due to external photon vertices at μ and ν. However, the required combination in the neutral channel,

$$[g_{\mu\nu}I(m_\pi^2,m_\pi^2;t)-J_{\mu\nu}(q_1,q_2)]$$
$$=\frac{i}{(4\pi)^2}\left\{2g_{\mu\nu}\int_0^1 d\alpha_1\int_0^1 d\alpha_2\,\theta(1-\alpha_1-\alpha_2)\ln(R/R_0)\right.$$
$$+\int_0^1 d\alpha_1\int_0^1 d\alpha_2\frac{\theta(1-\alpha_1-\alpha_2)}{R}[(2\alpha_1-1)q_{1\mu}$$
$$\left.+2\alpha_2 q_{2\mu}][2\alpha_1 q_{1\nu}+(2\alpha_2-1)q_{2\nu}]\right\}, \quad \text{(A4)}$$
$$R=m_\pi^2-(q_1^2\alpha_1+q_2^2\alpha_2)(1-\alpha_1-\alpha_2)-t\alpha_1\alpha_2,$$
$$R_0=m_\pi^2-t\alpha_2(1-\alpha_2),$$

is convergent.

(iii) The subleading in N_c^{-1} contribution in the charged channel requires the additional combination of integrals in Eq. (54) that arises from Fig. 2(c). They are given by the convergent expressions

$$J(k_1,k_2)=\int\frac{d^4l}{(2\pi)^4}$$
$$\times\frac{1}{[(l+k_1)^2-m_\pi^2][(l+k_2)^2-m_\pi^2][l^2-m_\sigma^2]}$$
$$=-\frac{i}{(4\pi)^2}\int_0^1 dx\,x\int_0^1 d\beta$$
$$\times\frac{1}{m_\sigma^2(1-x)+m_\pi^2x^2-tx^2\beta(1-\beta)} \quad \text{(A5)}$$

and

$$I_{\mu\nu}(q_1,k_1,k_2)=\int dl\frac{[2l+2k_1+q_1]_\mu[2l+2k_2+q_2]_\nu}{[(l+k_1)^2-m_\pi^2][(l+k_2)^2-m_\pi^2][(l+k_1+q_1)^2-m_\pi^2][l^2-m_\sigma^2]}$$
$$=-\frac{i}{(4\pi)^2}\int_0^1\prod_{i=1}^4(d\alpha_i)\,\delta\left(1-\sum_{j=1}^4\alpha_j\right)\left\{\frac{2g_{\mu\nu}}{R}-\frac{1}{R^2}[2\alpha_1k_1+2\alpha_4q_2+(2(\alpha_1+\alpha_3)-1)q_1]_\mu\right.$$
$$\left.\times[2\alpha_1k_1+2(\alpha_1+\alpha_3)q_1+(2\alpha_4-1)q_2]_\nu\right\}, \quad \text{(A6)}$$

where $R=m_\sigma^2\alpha_1+m_\pi^2(1-\alpha_1)^2-2k_1q_1\alpha_1\alpha_2-t\alpha_3(1-\alpha_1-\alpha_2-\alpha_3)$ for on-shell pions and photons.

[1] B. Holstein, Comments Nucl. Part. Phys. **19**, 221 (1990).
[2] T.A. Aibergenov *et al.*, Czech. J. Phys., Sect. B **36**, 948 (1986).
[3] Yu.M. Antipov *et al.*, Phys. Lett. **121B**, 445 (1983).
[4] Yu.M. Antipov *et al.*, Z. Phys. C **26**, 495 (1985).
[5] J. Boyer *et al.*, Mark II Collaboration, Phys. Rev. D **42**, 1350 (1990); H. Marsiske *et al.*, Crystal Ball Collaboration, *ibid.* **41**, 3324 (1990).
[6] H.–J. Behrend *et al.*, CELLO Collaboration, Z. Phys. C **56**, 381 (1992).
[7] A.E. Kaloshin and V.V. Serebryakov, Z. Phys. C **64**, 689 (1994).
[8] J. Portoles and M. R. Pennington, in *The Second DAΦNE Physics Handbook*, edited by L. Maiani, G. Pancheri, and N. Paver (INFN, Frascati, 1995), p. 579.
[9] S. Bellucci, J. Gasser, and M.E. Sainio, Nucl. Phys. **B423**, 80 (1994).
[10] V.N. Pervushin and M.K. Volkov, Phys. Lett. **58B**, 74 (1975); V. Bernard, B. Hiller, and W. Weise, Phys. Lett. B **205**, 16 (1988); D. Ebert and M.K. Volkov, Phys. Lett. **101B**, 252 (1981); M. Moreno and J. Pestieau, Phys. Rev. D **13**, 175 (1976); C-Y. Lee, *ibid.* **32**, 658 (1985).
[11] J. Bijnens and F. Cornet, Nucl. Phys. **B296**, 557 (1988).
[12] V. Bernard and D. Vautherin, Phys. Rev. D **40**, 1615 (1989).
[13] M.A. Ivanov and T. Mizutani, Phys. Rev. D **45**, 1580 (1992).
[14] V. Bernard, A.A. Osipov, and U.-G. Meissner, Phys. Lett. B **285**, 119 (1992).
[15] J. Bijnens, A. Fayyazuddin, and J. Prades, Phys. Lett. B **379**, 209 (1996); J. Bijnens and J. Prades, Nucl. Phys. **B490**, 239 (1997).
[16] B. Bajc, A.H. Blin, B. Hiller, M.C. Nemes, A.A. Osipov, and M. Rosina, Nucl. Phys. **A604**, 406 (1996).
[17] J. Hüfner, S.P. Klevansky, P. Rehberg, and M.K. Volkov, Z. Phys. C **75**, 127 (1997).
[18] A.E. Dorokhov *et al.*, Z. Phys. C **127**, 128 (1997).
[19] J. Gasser and H. Leutwyler, Ann. Phys. (N.Y.) **158**, 142 (1984).
[20] J.F. Donoghue and B.R. Holstein, Phys. Rev. D **40**, 2378 (1989).
[21] D. Babusci *et al.*, Phys. Lett. B **227**, 158 (1992).
[22] U. Bürgi, Phys. Lett. B **377**, 147 (1996).
[23] U. Bürgi, Nucl. Phys. **B479**, 392 (1996).
[24] V.A. Petrun'kin, Fiz. Elem. Chastits. At Yadra **12**, 692 (1981) [Sov. J. Part. Nucl. **12**, 278 (1981)]; L.V. Fil'kov, I. Guiasu, and E.E. Radescu, Phys. Rev. D **26**, 3146 (1982).
[25] J.F. Donoghue and B.R. Holstein, Phys. Rev. D **48**, 137 (1993).
[26] T. Das, V. Mathur, and S. Okubo, Phys. Rev. Lett. **19**, 859 (1967).
[27] S.P. Klevansky, R.H. Lemmer, and C.A. Wilmot, Phys. Lett. B **457**, 1 (1999).
[28] J.I. Kapusta and E.V. Shuryak, Phys. Rev. D **49**, 4694 (1994).
[29] R. Barate, ALEPH Collaboration, Z. Phys. C **76**, 15 (1997); Eur. Phys. J. C **4**, 431 (1998).
[30] M.J. Lavelle, N.F. Nasrallah, and K. Schilcher, Phys. Lett. B **335**, 211 (1994).
[31] W. Wilcox, Phys. Rev. D **57**, 6731 (1998).
[32] Y. Nambu, Phys. Rev. Lett. **4**, 380 (1960); Y. Nambu and G. Jona Lasinio, Phys. Rev. **122**, 345 (1961); **124**, 246 (1961); For extensive reviews of the properties of Nambu–Jona-Lasinio Lagrangians see, besides Ref. [33], U. Vogl and W. Weise, Prog. Part. Nucl. Phys. **27**, 195 (1991); T. Hatsuda and T. Kunihiro, Phys. Rep. **247**, 221 (1994); J. Bijnens, *ibid.* **265**, 369 (1996).
[33] S.P. Klevansky, Rev. Mod. Phys. **64**, 649 (1992).
[34] D. Ebert and M.K. Volkov, Z. Phys. C **16**, 205 (1983).
[35] M.K. Volkov, Ann. Phys. (N.Y.) **157**, 282 (1984); A. Dhar and S.R. Wadia, Phys. Rev. Lett. **52**, 959 (1984); A. Dhar, R. Shankar, and S.R. Wadia, Phys. Rev. D **31**, 3256 (1985); D. Ebert and H. Reinhardt, Nucl. Phys. **B27**, 188 (1986).
[36] S.B. Gerasimov, Yad. Fiz. **29**, 513 (1979) [Sov. J. Nucl. Phys. **29**, 259 (1979)].
[37] P. Langacker and H. Pagels, Phys. Rev. D **8**, 4620 (1973); W. Marciano and H. Pagels, Phys. Rep. **36**, 137 (1978).
[38] R. Tarrach, Z. Phys. C **12**, 221 (1979).
[39] See, for example, C. Itzykson and J. Zuber, *Quantum Field Theory* (McGraw-Hill, New York, 1980).
[40] J. Müller and S.P. Klevansky, Phys. Rev. C **50**, 410 (1994).
[41] R. Dashen, Phys. Rev. **183**, 1245 (1969).
[42] V. Dmitrasinovic, H.-J. Schulze, R. Tegen, and R.H. Lemmer, Phys. Rev. D **52**, 2855 (1995).
[43] J.F. Donoghue and E. Golowich, Phys. Rev. D **49**, 1513 (1994).
[44] T.E.O. Ericson and J. Hüfner, Nucl. Phys. **B57**, 604 (1973).
[45] S. Klimt, M. Lutz, U. Vogel, and W. Weise, Nucl. Phys. **A516**, 429 (1990).
[46] S. Gasiorowicz and D.A. Geffen, Rev. Mod. Phys. **41**, 531 (1969).
[47] R.H. Lemmer and C.A. Wilmot, Nucl. Phys. **A690**, 263c (2001).
[48] V. Bernard, A.A. Osipov, and U.-G. Meissner, Phys. Lett. B **292**, 205 (1992).